Title

Complexation of NpO2 + with Amine-Functionalized Diacetamide Ligands in Aqueous Solution: Thermodynamic, Structural, and Computational Studies

Journal

Inorganic Chemistry, 57(12)

ISSN

0020-1669

Authors

Gao, Yang
Dau, Phuong V
Parker, Bernard F
et al.

Publication Date

2018-06-18

DOI

10.1021/acs.inorgchem.8b00654

Peer reviewed

Inorganic Chemistry
Cite This: Inorg. Chem. 2018, 57, 6965−6972
Article
pubs.acs.org/IC

Complexation of NpO_2^+ with Amine-Functionalized Diacetamide Ligands in Aqueous Solution: Thermodynamic, Structural, and Computational Studies

Yang Gao,[†,‡] Phuong V. Dau,[†] Bernard F. Parker,[†,§] John Arnold,[†,§] Andrea Melchior,*[,∥] Zhicheng Zhang,*[,†] and Linfeng Rao*[,†]

[†]Chemical Sciences Division, Lawrence Berkeley National Laboratory, 1 Cyclotron Road, Berkeley, California 94720, United States
[‡]College of Nuclear Science and Technology, Harbin Engineering University, 150001 Harbin, China
[§]Department of Chemistry, University of California−Berkeley, Berkeley, California 94720, United States
[∥]Dipartimento Politecnico di Ingegneria e Architettura, Università di Udine, Laboratori di Chimica, via delle Scienze 99, 33100 Udine, Italy

Supporting Information

ABSTRACT: Complexation of Np(V) with three structurally related amine-functionalized diacetamide ligands, including 2,2′-azanediylbis(*N*,*N*′-dimethylacetamide) (ABDMA), 2,2′-(methylazanediyl)bis(*N*,*N*′-dimethylacetamide) (MABDMA), and 2,2′-(benzylazanediyl)bis(*N*,*N*′-dimethylacetamide) (BnABDMA), in aqueous solutions was investigated. The stability constants of two successive complexes, namely, NpO_2L^+ and $NpO_2L_2^+$, where L stands for the ligands, were determined by absorption spectrophotometry. The results suggest that the stability constants of corresponding Np(V) complexes follow the trend: MABDMA > ABDMA ≈ BnABDMA. The data are discussed in terms of the basicity of the ligands and compared with those for the complexation of Np(V) with an ether oxygen-linked diacetamide ligand. Extended X-ray absorption fine structure data indicate that, similar to the complexation with Nd^{3+} and UO_2^{2+}, the ligands coordinate to NpO_2^+ in a tridentate mode through the amine nitrogen and two oxygen atoms of the amide groups. Computational results, in conjunction with spectrophotometric data, verify that the 1:2 complexes ($NpO_2(L)_2^+$) in aqueous solutions are highly symmetric with Np at the inversion center, so that the f−f transition of Np(V) is forbidden and $NpO_2(L)_2^+$ does not display significant absorption in the near-IR region.

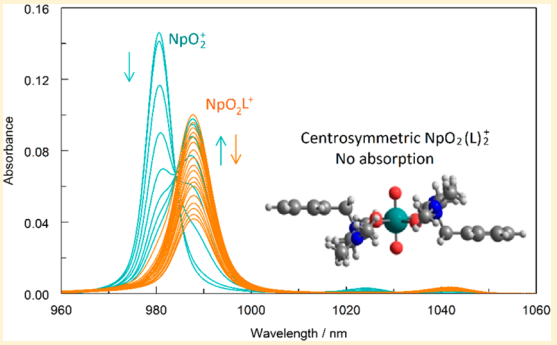

1. INTRODUCTION

Neptunium is one of the most problematic elements in the reprocessing process of spent nuclear fuel (SNF) as well as in the environmental management of high-level nuclear wastes (HLW) due to its redox and extraction behavior in reprocessing and its transport characteristics in the geological environment. Because of its long half-life, $t_{1/2} = 2.144 \times 10^6$ years, ^{237}Np is predicted to contribute 67% of the total radiation dose from HLW after 75 000 years of storage in the respository.[1] Also, the pentavalent state of neptunium, Np(V), is the most stable state and exists as NpO_2^+ ions in aqueous solution. Possessing a low ionic charge and relatively large ionic radius, NpO_2^+ does not hydrolyze in weakly acidic or neutral solutions, resulting in high solubility and mobility in the waste repository. Besides, complexation of NpO_2^+ with many ligands is weak, and its extraction by many traditional extracts in actinide separation processes is difficult. It is of prime importance to explore ligands that can strongly bind NpO_2^+ and separate it from high-level nuclear wastes, helping to improve the safe management of waste repositories.

There have been a number of studies on the complexation of organic ligands with neptunium, including monocarboxylic acids such as benzoic acid[2] and picolinic acid,[3] dicarboxylic acids such as dipicolinic acid (H_2DPA),[4] 1,10-phenanthroline-2,9-dicarboxylic acid ($H_2PhenDA$),[5] iminodiacetic acid (IDA),[6,7] and *N*-methyliminodiacetic acid (MIDA),[8,9] and glutaroimide-dioxime.[10] These ligands, while exhibiting fairly good complexation capabilities with Np(V), are completely combustible, because they contain only C, H, O, and N atoms. As a result, use of these ligands could help to significantly reduce the volume of solid radioactive wastes in the separation processes.

In recent years, alkyl-substituted diglycolamides have been studied as efficient complexants for separations of actinides and lanthanides in SNF reprocessing.[10] Diglycolamides contain an ether oxygen linkage between two amide groups and usually form tridentate complexes with metal ions using the three oxygen donor atoms from the ether and the two amide groups. Use of these ligands (also containing only C, H, O, and N atoms) helps to improve the environmental sustainability of the separation processes. Additionally, by varying the substitutional groups on

Received: March 12, 2018
Published: June 5, 2018

DOI: 10.1021/acs.inorgchem.8b00654
Inorg. Chem. 2018, 57, 6965−6972

the amide nitrogen, diglycolamides can be used either as efficient extractants for solvent extraction, such as *N,N,N′,N′*-tetraoctyl-diglycolamide (TODGA)[11] and *N,N,N′,N′*-tetraisobutyl-diglycolamide (TiBDGA),[12] or as small molecules for single-phase thermodynamic studies such as *N,N,N′,N′*-tetramethyl-diglycolamide (TMDGA).[13]

By replacing the ether oxygen linkage in diglycolamides with an amine linkage, we designed and prepared three diacetamide ligands, including 2,2′-azanediylbis(*N,N′*-dimethylacetamide) (ABDMA), 2,2′-(methylazanediyl)bis(*N,N′*-dimethylacetamide) (MABDMA), and 2,2′-(benzylazanediyl)bis(*N,N′*-dimethylacetamide) (BnABDMA; Figure 1). The equilibrium

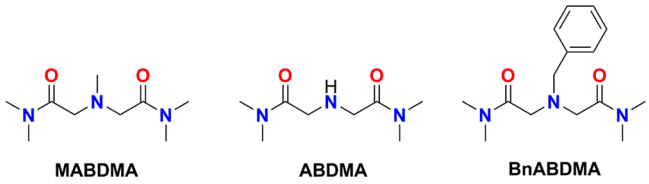

Figure 1. Structures of ABDMA, MABDMA, and BnABDMA.

constants and enthalpy of complexation between these ligands and metal ions including Nd(III)[14] and U(VI)[15] were determined. Using the amine nitrogen linkage in these ligands to replace the ether oxygen linkage in diglycolamides, we are able to fine-tune the basicity and metal-binding strength of the ligands through the substitution with various functional groups on the amine N atom. This "tunability" is not feasible for the ligands with the ether linkage such as TMDGA. The data for the complexation with Nd(III)[14] and U(VI)[15] show that the stability of the complexes follows the trend: MABDMA > ABDMA > BnABDMA, agreeing with the order of the basicity of the nitrogen donor atom in these ligands. It is the focus of the present study to extend the thermodynamic studies to NpO_2^+ and compare the data with those for Nd^{3+} and UO_2^{2+}.

One interesting feature of the complexation of NpO_2^+ with the ether oxygen linked diacetamide ligand TMDGA is that the 1:2 complex $NpO_2(L)_2^+$, where L = TMDGA, is "silent" in near-IR absorption spectroscopy,[13] which suggests the complex is centrosymmetric and the Np atom is at the inversion center so that the f−f transition is forbidden by the Laporte's rule.[16] The "silent" feature in absorption spectroscopy of NpO_2^+ has also been theoretically discussed in the literature.[17−20] In the case of the $NpO_2(L)_2^+$ complex with the amine-functionalized diacetamides (where L = BnABDMA, ABDMA, or MABDMA), the two ligands could be in a cis or trans configuration with respect to the equatorial plane of NpO_2^+, resulting in the absence or presence of an inversion center. Therefore, it is fundamentally interesting to determine, in addition to thermodynamic data, the optical absorption properties of the complexes and correlate these with the symmetry of the complexes.

In this work, the stability constants of the NpO_2^+ complexes with BnABDMA, ABDMA, and MABDMA were determined by spectrophotometry. The data are compared with those of Nd^{3+} and UO_2^{2+} in the literature. Extended X-ray absorption fine structure (EXAFS) and computational studies were conducted to help interpret the data and correlate the optical properties with the structure and symmetry of the NpO_2^+ complexes.

2. EXPERIMENTAL SECTION

2.1. Chemicals. Chemicals used in this work are all reagent grade or higher. 2,2′-azanediylbis(*N,N′*-dimethylacetamide) (ABDMA), 2,2′-(methylazanediyl)bis(*N,N′*-dimethylacetamide) (MABDMA), and 2,2′-(benzylazanediyl)bis(*N,N′*-dimethylacetamide) (BnABDMA) were synthesized according to previous procedures.[14] In preparing the ligands, commercially available materials (2-chloro-*N,N′*-dimethylacetamide, benzylamine, K_2CO_3, KI, and methylamine) and solvents (CH_3Cl and EtOH) were purchased from Sigma-Aldrich, TCI, EMD, and Alfa Aesar, and used without additional purification.

Boiled Milli-Q water was used in the preparation of all solutions. All experiments were conducted at 25 °C and an ionic strength of 1.0 M $NaNO_3$. The ionic medium of $NaNO_3$, instead of $NaClO_4$, was chosen for this work, because the solubility of the metal complexes with the diacetamide ligands is low in $NaClO_4$ solutions. The stock solution of Np(V) was prepared by following procedures as described elsewhere.[21] The concentration of Np(V) was determined by the absorbance at 980.2 nm (ε = 395 M^{-1} cm^{-1}), and the concentration of free acid in the stock solution was determined by Gran's titration.[22] ***Caution!*** *Neptunium is a radioactive material with α-radiation that presents significant hazards to human health and environment. Extreme precautions should be taken when handling this material.* Stock solutions of the three ligands were prepared by direct dissolution of proper quantities of the ligands in 1.0 M $NaNO_3$. The ligand concentration in the stock solution was obtained from the weight and verified by potentiometric titrations.

2.2. Spectrophotometry. Spectrophotometric titrations on a Cary 6000i UV−vis−NIR (NIR = near-infrared) spectrophotometer (Varian Inc.) were performed to obtain the stability constants of the complexes between NpO_2^+ and the three ligands. A 10 mm cuvette was used, and the slit width of the instrument was set to achieve 1 nm spectral bandwidth. The sample temperature was controlled at (25.0 ± 0.1) °C by a constant-temperature controller associated with the instrument. Absorption spectra were collected from 1065 to 950 nm stepwise with a 0.2 nm interval. In each titration, the initial solution (2.10 mL) containing NpO_2^+ was titrated by adding appropriate aliquots of ligand solution and mixing thoroughly for ∼2 min prior to the collection of spectra. The mixing time is sufficient, because preliminary experiments demonstrated that it required only 30 s to achieve complexation equilibrium. Usually, 20 or more additions of the titrant were made, and a set of 21 or more spectra were generated in each titration. Two titrations with different [Np(V)] were conducted (Table S1 of Supporting Information). The equilibrium constants were calculated by fitting the spectra with a commercial program HypSpec.[23]

Prior to the spectrophotometric titrations, scoping tests were conducted to confirm that the optical absorption of either $NaNO_3$ or the ligands in the wavelength region is negligible and to help select the optimal concentrations of neptunium and acidity for the titrations. On the basis of the results from scoping tests, the initial [Np] in the cuvette was selected to be 0.3−0.4 mM, resulting in optical absorbance of 0.12−0.16 at 980 nm and high-quality spectra on the Cary-6000i spectrometer. Using higher [Np] in the titrations was not desirable because of two reasons: (1) it would require higher concentrations of the ligand to achieve a high ratio of ligand/metal, which could lead to cloudiness of the sample solution as observed in preparing the EXAFS samples in this work; and (2) it would present more hazards and increase radioactive waste.

The neutral diamide ligands, protonated diamide ligands, and the NpO_2^+/diamide complexes are denoted in this paper as L, HL^+, and $NpO_2(L)_j^+$, respectively, where j = 1 and 2.

2.3. EXAFS. Seven Np(V) solution samples were prepared, and the EXAFS spectra were collected at Stanford Synchrotron Radiation Laboratory. Solution I did not contain any ligands and represents the free NpO_2^+ ion. Sample solutions II−VII consisted of Np(V) and the ligands at different concentrations and acidities such that either $NpO_2(L)^+$ or $NpO_2(L)_2^+$ was the dominant complex in a sample. The speciation of Np(V) species in sample solutions II−VII was calculated using the complexation equilibrium constants from this work and shown in Figure S1 of Supporting Information.

Each solution sample (2 mL) was placed in a polyethylene vial that was doubly sealed in two plastic bags. The samples were attached to a sample positioner with adhesive tape, and EXAFS data collected on Beamline 11−2 at neptunium L_{III}-edge up to $k_{max} \approx 14$ Å^{-1} in

DOI: 10.1021/acs.inorgchem.8b00654
Inorg. Chem. 2018, 57, 6965−6972

transmission and fluorescence modes. For each sample, three to four scans were usually taken.

Yttrium foil was used as the reference in the measurements. Therefore, energy calibration was accomplished by assigning the first inflection point of the K edge of yttrium at 17 038 eV. Program Athena[24] was used to perform data reduction, including the subtraction of pre-edge background, spline fitting, and normalization. The threshold energy E_0 was defined as 17 166 eV, above which the EXAFS spectra were extracted. The program FEFF7[25] was used to calculate the theoretical phases and amplitudes, starting with the crystal structure of $UO_2L_2(ClO_4)_2$ (CCDC 1584249), where L stands for 2,2′-(trifluoroazanediyl)bis(*N*,*N*′-dimethylacetamide) and elongating the U−N and U−O bonds in this structure for corresponding Np−N and Np−O bonds. Then the calculated theoretical phases and amplitudes were used for fitting the EXAFS data. In all the fits, EXAFS spectra with a k range (3.0−14.0 Å^{-1}) and Fourier transform magnitudes with an R range (0.95−3.5 Å) were used, while considering the amplitude factor (S_0^2) and the threshold energy shift (ΔE_0) as global parameters.

2.4. Computation. Density functional theory (DFT) calculations were performed on the complexes and ligands at the level of three-parameter hybrid functional B3LYP.[26,27] This level of theory has previously been shown to generate reliable data of structure and energy of actinide complexes.[15,28,29] Grimme's D3 empirical dispersion correction[30] was also employed, as it has been demonstrated to be important when calculating the binding energies of ligands of different bulkiness.[31] Stuttgart−Dresden small-core quasi-relativistic effective core potentials were employed for neptunium.[32] A 6-31++G(d,p) Gaussian-type basis set was used to treat other elements. Solvent effect was accounted for by utilizing the polarizable continuum model (PCM).[33] Geometry optimizations of the $NpO_2(L)_2^+$ complexes were run with symmetry constraints in PCM solvent (the point groups are reported with the optimized structures in the section of Results). The free energies of the complexes were calculated by adding to the electronic energy of each complex the zero point energy as well as the thermal corrections that include the contribution of electronic, harmonic vibrational, rotational, and translational energies to the internal energy. All calculations were performed with Gaussian16.[34]

3. RESULTS AND DISCUSSION

3.1. Stability Constants of Np(V) Complexes with ABDMA, BnABDMA, and MABDMA. A representative set of absorption spectra for the titration of Np(V) with MABDMA is shown in Figure 2. The variations of spectra along the titration

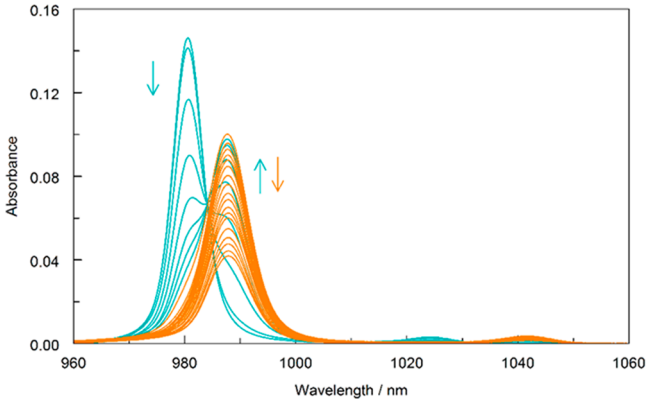

Figure 2. Spectrophotometric titration of NpO_2^+ complexation with MABDMA (I = 1.0 M $NaNO_3$, t = 25 °C). Initial concentrations in cuvette: C_{Np} = 0.386 mM, C_H = 0.443 mM, $C_{nitrate}$ = 1.00 M; titrant: C_L = 38.0 mM, $C_{nitrate}$ = 1.00 M. The variations of the spectra during the titration are discussed in two phases: Phase I (cyan color) and Phase II (orange color).

can be described in two phases: (1) Phase I (cyan color), where the intensity of the absorption band of free NpO_2^+ around 980 nm decreases, and a new band appears at 988 nm and intensifies as the concentration of ligand increases, indicating the formation of a Np(V) complex (probably a 1:1 complex); and (2) Phase II (orange color), where the intensity at 988 nm decreases, but no new absorption peaks appear at longer wavelengths.

These observations are different from those for Np(V) complexes with many ligands (e.g., oxalate, fluoride, sulfate, picolinate, glutaroimide-dioxime), where the decrease of the absorbance of the first complex is accompanied by the appearance of new absorption band(s) of successive complexes at longer wavelengths,[3,10,35−37] but they are very similar to those for the ligands that form centrosymmetric 1:2 Np(V) complexes (e.g., DPA, TMDGA, MIDA, ODA).[4,9,13,38,39] Accordingly, the spectrophotometric titration data could be interpreted as showing the successive formation of the 1:1 and 1:2 Np(V)/L complexes (reactions 1 and 2), with the 1:1 complex absorbing at 988 nm and the 1:2 complex not absorbing in the experimental wavelength region. This interpretation is consistent with the spectra factor analysis that suggests, besides the free NpO_2^+ and $NpO_2(NO_3)_{(aq)}$ complex, there is only one additional absorbing species, that is, presumably, the 1:1 $NpO_2(L)^+$ complex in the solutions.

$$NpO_2^+ + L = [NpO_2L]^+ \quad (1)$$

$$NpO_2L^+ + L = [NpO_2L_2]^+ \quad (2)$$

The variations of spectra in the spectrophotometric titrations with all three ligands are similar and shown in Figure 3. The first

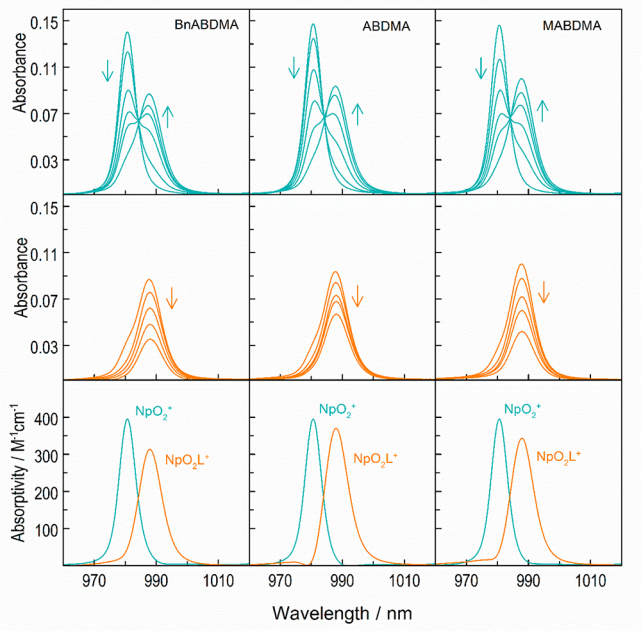

Figure 3. Analysis of spectrophotometric titration data for the complexation of NpO_2^+ with BnABDMA, ABDMA, and MABDMA. The first row: Phase I of the titration showing the decrease of free NpO_2^+ and the formation of $NpO_2(L)^+$; the second row: Phase II of the titration showing the decrease of $NpO_2(L)^+$ with no new absorption bands for the formation of $NpO_2(L)_2^+$; the third row: molar absorptivities of NpO_2^+ and $NpO_2(L)^+$; the molar absorptivity of NpO_2NO_3 is omitted for clarity.

row of Figure 3 represents Phase I of the titrations, where the formation of $NpO_2(L)^+$ is dominant (reaction 1), while the second row represents Phase II of the titrations, where the formation of $NpO_2(L)_2^+$ is dominant (reaction 2). The third row shows the calculated molar absorptivities of the $NpO_2(L)^+$ complexes.

DOI: 10.1021/acs.inorgchem.8b00654
Inorg. Chem. 2018, 57, 6965−6972

Various models were tested to fit the spectrophotometric data, including the model with the formation of two successive Np(V) complexes ($NpO_2(L)^+$ and $NpO_2(L)_2^+$), the model with protonated Np(V) complexes such as $NpO_2(HL)^{2+}$, and the model with hydrolyzed Np(V) species such as $NpO_2(OH)$. Best fit of the spectra was obtained by fitting the data with the model including the formation of two successive NpO_2^+ complexes as shown by reactions 1 and 2, and the calculated equilibrium constants are shown in Table 1, in comparison with the constants

Table 1. Equilibrium Constants for the Protonation and Complexation of ABDMA, BnABDMA, and MABDMA, with NpO_2^+ at 25 °C and I = 1.0 M $NaNO_3$

ligand	reaction	method[a]	log β	ref[b]
BnABDMA	$H^+ + L = HL^+$	pot, cal	6.36 ± 0.09	14
	$NpO_2^+ + L = NpO_2(L)^+$	sp	2.90 ± 0.09	pw
	$NpO_2^+ + 2L = NpO_2(L)_2^+$	sp	4.01 ± 0.09	
ABDMA	$H^+ + L = HL^+$	pot, cal	7.12 ± 0.09	14
	$NpO_2^+ + L = NpO_2(L)^+$	sp	2.80 ± 0.09	pw
	$NpO_2^+ + 2L = NpO_2(L)_2^+$	sp	4.00 ± 0.09	
MABDMA	$H^+ + L = HL^+$	pot, cal	7.64 ± 0.09	14
	$NpO_2^+ + L = NpO_2(L)^+$	sp	3.59 ± 0.09	pw
	$NpO_2^+ + 2L = NpO_2(L)_2^+$	sp	5.50 ± 0.09	
TMDGA	$NpO_2^+ + L = NpO_2(L)^+$	sp	1.37 ± 0.01	13
	$NpO_2^+ + 2L = NpO_2(L)_2^+$	sp	2.47 ± 0.01	

[a]Methods: pot—potentiometry, cal—calorimetry, sp—spectrophotometry. [b]pw = present work.

for the complexation of NpO_2^+ with TMDGA from the literature.[13] When fitting the data with the model including the hydrolysis of Np(V), two values of the hydrolysis constant ($\log(*\beta_1) = -9.06$[21] or -11.13[40] from the literature, where $*\beta_1$ is the hydrolysis constant for the reaction $NpO_2^+ + H_2O = NpO_2(OH) + H^+$) were tested. The $NpO_2(OH)$ species in the final cuvette solution ranges from 0.5% to 1.5% by using the value of −9.06, but it is nearly 0% by using the value of −11.13. The calculated equilibrium constants for the complexation reactions 1 and (2) remain unchanged whether the hydrolysis is included or excluded. The speciation information concerning the hydrolysis was provided together with the titration conditions in Table S1 of Supporting Information.

3.2. Comparison of the Binding Strength among the Three Amine-Functionalized Diacetamides. For both $NpO_2(L)^+$ and $NpO_2(L)_2^+$ complexes, the binding strength of the three ligands follows the order: MABDMA > ABDMA ≈ BnABDMA. This order is in fair agreement with those observed for the complexation with Nd(III)[14] and U(VI),[15] where MABDMA > ABDMA > BnABDMA. These trends are interpreted as reflecting the complexation reactions are predominantly electrostatic interactions: the electron-donating methyl group increases and the electron-withdrawing benzyl group decreases the electron density on the amine nitrogen, resulting in stronger metal complexes with MABDMA than those with BnABDMA and ABDMA.

3.3. Comparison of the Binding Strength between the Amine-Linked Ligands and Ether Oxygen-Linked TMDGA. As shown in Table 1, all three amine-linked ligands form stronger complexes with NpO_2^+ than the ether oxygen-linked TMDGA. Such a trend is often observed when comparing the binding strength between nitrogen-donor and analogous oxygen-donor ligands in aqueous solution. For example, metal complexes with iminodiacetic acid (IDA) are stronger than those with oxidiacetic acid (ODA).[41] The difference in binding is usually attributed to the higher basicity and less hydration of amine/imine nitrogen than ether oxygen in aqueous solutions, supported by the difference in the enthalpy and entropy of complexation between the two groups of ligands in the complexation of metal ions.

3.4. Identification of Np(V) Complexes in Solution by EXAFS. No EXAFS data for Sample VII (Figure S1 of Supporting Information) were obtained, because this sample was found cloudy. The EXFAS spectra (k^3-weighted) and Fourier transform magnitude of Samples I–VI are shown in Figure 4. The fitting results are summarized in Table 2.

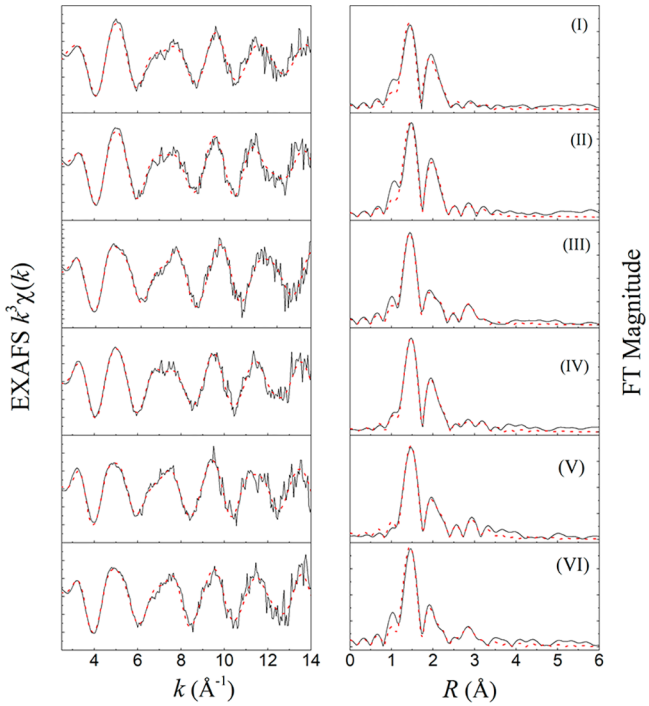

Figure 4. (left) k^3-weighted EXAFS spectra; (right) Fourier transfer magnitudes.

The structural parameters of the Np species in solution samples (I–VI) obtained by EXAFS are shown in Table 2. For the free NpO_2^+ ion (Solution I), five oxygen atoms (from water molecules) were identified in the equatorial plane, consistent with observation in the literature.[41,42] For the solutions where the $NpO_2(L)^+$ complexes are dominant (solutions II and IV), one nitrogen atom and four oxygen atoms in the equatorial plane were observed, suggesting there is one ligand and two water molecules coordinating to Np and the ligand is tridentate using the amine nitrogen and two oxygen atoms from the amide groups. For the solutions where the $NpO_2(L)_2^+$ complexes are dominant (solutions III, V, and VI), two nitrogen atoms and four oxygen atoms in the equatorial plane were observed, suggesting there are two ligand molecules coordinating to Np and, same as in the $NpO_2(L)^+$ complexes, the ligand is tridentate using the amine nitrogen and two oxygen atoms from the amide groups.

The EXAFS data provide evidence that, despite its "silent" feature in the absorption spectra, the 1:2 complexes $NpO_2(L)_2^+$ are in fact present in solutions where the ligand/metal ratio is high.

3.5. Symmetry and Optical Absorption: Computational Data. Minimum energy structures of each $NpO_2L_2^+$ complex (L = ABNMA, MABDMA, and BnABDMA) were obtained for three types of isomers as shown in three columns of Figure 5.

DOI: 10.1021/acs.inorgchem.8b00654
Inorg. Chem. 2018, 57, 6965–6972

Table 2. EXAFS Data of Np(V) Species in Solution Samples (I–VI)

solution[a]	shell	N^b	R (Å)	σ^2	notice[c]
I (free Np(V))	Np–O_{ax}	2.0	1.82 ± 0.01	0.0025	S_0^2 = 1.0, ΔE^0 = 9.5 eV
100% NpO_2^+	Np–O_{eq}	4.9 ± 1.1	2.46 ± 0.02	0.0043	r = 0.0017
II (Np(V)/MABDMA)	Np–O_{ax}	2.0	1.82 ± 0.01	0.0019	S_0^2 = 1.0, ΔE^0 = 8.4 eV
15% NpO_2^+	Np–O_{eq}	4.1 ± 1.0	2.45 ± 0.04	0.0042	r = 0.0067
75% $NpO_2(L)^+$					
10% $NpO_2(L)_2^+$	Np–N_{eq}	1.0 ± 0.2	3.02 ± 0.13	0.0036	
III (Np(V)/MABDMA)	Np–O_{ax}	2.0	1.82 ± 0.01	0.0018	S_0^2 = 1.0, ΔE^0 = 8.9 eV
10% $NpO_2(L)^+$	Np–O_{eq}	3.9 ± 1.0	2.49 ± 0.04	0.0051	r = 0.0030
90% $NpO_2(L)_2^+$	Np–N_{eq}	2.0 ± 0.4	3.05 ± 0.10	0.0041	
IV (Np(V)/ABDMA)	Np–O_{ax}	2.0	1.81 ± 0.01	0.0017	S_0^2 = 0.86, ΔE^0 = 8.8 eV
10% NpO_2^+	Np–O_{eq}	4.3 ± 1.1	2.45 ± 0.02	0.0086	r = 0.0021
75% $NpO_2(L)^+$	Np–N_{eq}	1.1 ± 0.2	3.11 ± 0.10	0.0027	
15% $NpO_2(L)_2^+$					
V (Np(V)/ABDMA)	Np–O_{ax}	2.0	1.82 ± 0.02	0.0019	S_0^2 = 0.93, ΔE^0 = 8.9 eV
10% $NpO_2(L)^+$	Np–O_{eq}	4.1 ± 0.8	2.48 ± 0.05	0.0049	r = 0.0055
90% $NpO_2(L)_2^+$	Np–N_{eq}	1.9 ± 0.4	3.10 ± 0.09	0.0035	
VI (Np(V)/BnABDMA)	Np–O_{ax}	2.0	1.82 ± 0.02	0.0017	S_0^2 = 1.0, ΔE^0 = 8.9 eV
5% $NpO_2(L)^+$	Np–O_{eq}	3.9 ± 0.8	2.47 ± 0.06	0.0052	r = 0.043
95% $NpO_2(L)_2^+$	Np–N_{eq}	1.9 ± 0.4	3.07 ± 0.11	0.0045	

[a]The speciation of Np(V) (percentages of total [Np]) was calculated by using the complexation constants that were determined in this work. [b]The number of Np–O_{ax} path was held constant in the fit of all samples. [c]r is the fit factor as an indicator of the fit quality.

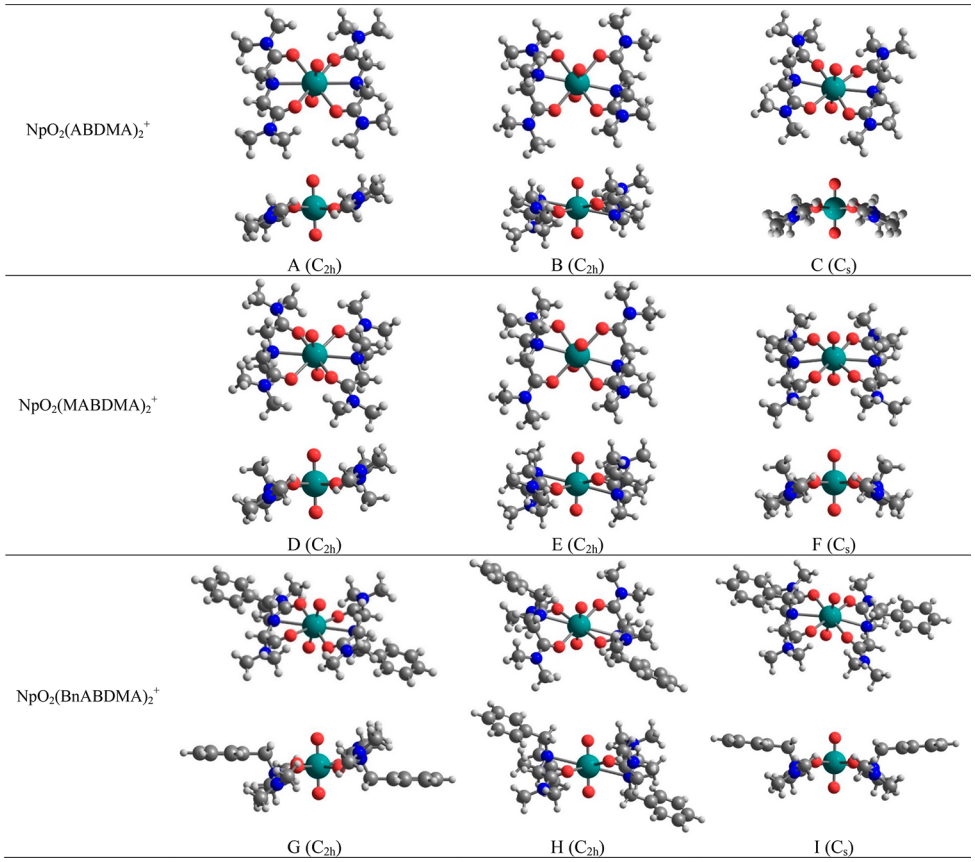

Figure 5. Calculated minimum energy structures and the molecular point groups of the $NpO_2(L)_2^+$ complexes. For each complex, the upper row represents the structures viewed from the top of the equatorial plane of NpO_2^+, and the lower row represents the structures viewed along the equatorial plane of NpO_2^+. Two types of centrosymmetric isomers (A, D, G in the first column and B, E, H in the second column) and one type of noncentrosymmetric isomers (C, F, I in the third column) are represented. A, B, and C are for $NpO_2(ABDMA)_2^+$ complex; D, E, and F are for $NpO_2(MABDMA)_2^+$ complex; G, H, and I are for $NpO_2(BnABDMA)_2^+$ complex.

Two types of centrosymmetric isomers are represented, respectively, in the first column (A, D, and G) and in the second column (B, E, and H). These two types of isomers were previously shown to be present in similar U(VI) systems.[15] The third type of isomers are noncentrosymmetric and shown in the third column of Figure 5 (C, F, and I).

The structures in the first and the second columns of Figure 5 are centrosymmetric (C_{2h} point group) with the Np atom at the

DOI: 10.1021/acs.inorgchem.8b00654
Inorg. Chem. 2018, 57, 6965–6972

Table 3. Relative Free Energy[a] ΔG of the Structures of $NpO_2(L)_2^+$ Complexes in Aqueous Solution

Complex		Structure	ΔG_{water}, kJ·mol^{-1}
$NpO_2(ABDMA)_2^+$	A (C_{2h})	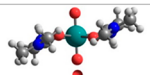	0.0
	C (C_s)	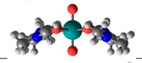	8.4
$NpO_2(MABDMA)_2^+$	D (C_{2h})	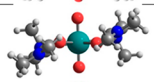	0.0
	F (C_s)	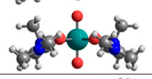	5.2
$NpO_2(BnABDMA)_2^+$	G (C_{2h})	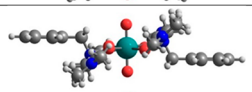	0.0
	I (C_s)	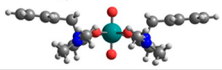	22.2

[a]Calculated at the B3LYP-D3 level.

inversion center. They both have the substitutional groups of the two ligands on the central amine N (e.g., the benzyl group in BnABDMA, the methyl group in MABDMA, and the hydrogen in ABDMA) in the trans position, but they differ in the arrangements of the " >N−C(O)−C−N−C−C(O)−N< " backbone with respect to the equatorial plane of NpO_2^+. The diacetamide ligands are nearly planar (the O−C···C−O dihedral angles ~0°) in the structures of the first column (Structures A, D, G), while the diacetamide ligands are nonplanar (O−C···C−O dihedral angles ~30°) in the structures of the second column (Structures B, E, H). Selected bond lengths of the structures calculated at both B3LYP and B3LYP-D3 levels are reported in Table S2 and compared with the experimentally observed bond lengths from EXAFS. As shown in Table S2, the calculated Np−O_{ax} bond length is in excellent agreement with the EXAFS data for all complexes. However, note that, for all three ML_2 complexes, the calculated Np−O_{eq} bonds are ~0.06−0.13 Å longer than those from EXAFS. On the contrary, the calculated Np−N bonds are systematically shorter (by ~0.07−0.36 Å, with an average of 0.24 Å) than those from EXAFS. Such difference between the calculated and EXAFS measured bond lengths has been observed for similar amine-linked diamide complexes with UO_2^{2+} in a previous study.[15] Different functionals (B3LYP and B3LYP-D3) seem to generate similar bond lengths with similar trends of overestimating the equatorial M−O bonds while underestimating the equatorial M−N bond lengths (Table S2). Without a satisfactory explanation for this observation, we note that, while the differences in $R_{Np\text{-}Oeq}$ between the calculated and the experimental values (Δr) are similar for all three $NpO_2(L)_2^+$ complexes, the difference in R_{Np-N} between the calculated and the experimental values (Δr) for the $NpO_2(ABDMA)_2^+$ complexes is significantly larger than those for the $NpO_2(MABDMA)_2^+$ and $NpO_2(BnABDMA)_2^+$ complexes (Table S2). Therefore, we hypothesize that the presence of additional water H-bonds to the amine group of ABDMA could have a significant effect on the Np−N bond length.

Calculations at the B3LYP-D3 level indicate that the structures in the first column (A, D, and G) always possess lower energies than those in the second column (B, E, and H) in aqueous media: the B, E, and H structures are less stable than A, D, and G by ~8, 10, and 31 kJ/mol, respectively. Therefore, the following discussion on the comparison of energy between the centrosymmetric and noncentrosymmetric complexes is focused on the structures in the first column (centrosymmetric A, D, and G) and the third column (noncentrosymmetric C, F, and I).

The calculated energies of the noncentrosymmetric structures (C, F, and I) relative to those of the centrosymmetric structures (A, D, and G) are shown in Table 3. For the 1:2 complexes of NpO_2^+ with ABNMA, MABDMA, and BnABDMA, the noncentrosymmetric structures (C, F, and I) possess energies higher than the centrosymmetric structures (A, D, and G) by 5.2, 8.4, and 22.2 kJ·mol^{-1}, respectively. This means that the $NpO_2(L)_2^+$ complexes in aqueous solution are most likely to be centrosymmetric.

The near-IR absorption bands of NpO_2^+ are known to originate from the f−f transitions that are electric-dipole forbidden according to Laporte's rule. A number of studies on NpO_2^+ complexes have demonstrated that the f−f transitions of Np(V) in a centrosymmetric structure where the Np atom sits at the inversion center are completely forbidden, and no absorption bands in the near-IR region are observed.[38,43,44] Only if the inversion center is destroyed by the arrangement of ligands surrounding NpO_2^+, absorption bands of Np(V) in the near-IR region can be observed. Integrating the experimental data from spectrophotometric titrations, the structural data from EXAFS, and the theoretical DFT calculated results in this work, the schematic structures and associated absorption characteristics of the Np(V) species, including the free NpO_2^+ and Np(V)/MABDMA complexes, can be described in Figure 6.

The free aquo NpO_2^+ ion and the 1:1 $NpO_2(L)^+$ complex show optical absorption bands at 980.6 and 987.8 nm, respectively, indicating that neither NpO_2^+ nor $NpO_2(L)^+$ is centrosymmetric. For the free $NpO_2(aq)^+$ ion, X-ray absorption in this study (Table 2) and other studies[41,42] has demonstrated

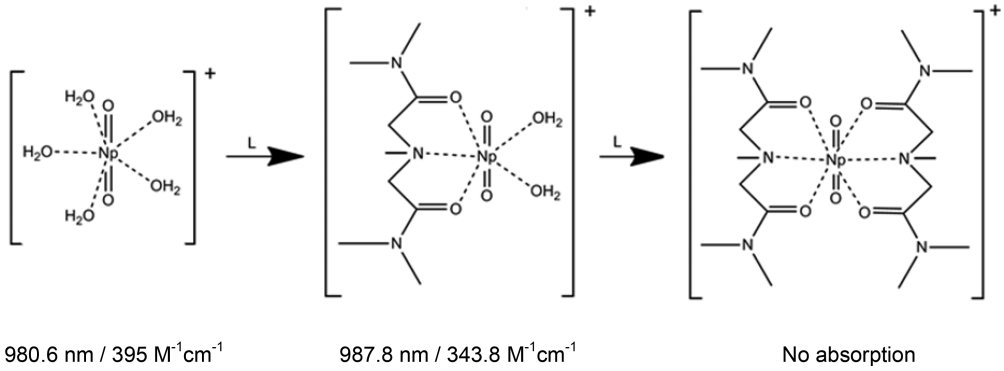

Figure 6. Stepwise complexation of NpO_2^+ with MABDMA and associated optical absorption characteristics (band wavelength/molar absorptivity) from this work.

DOI: 10.1021/acs.inorgchem.8b00654
Inorg. Chem. 2018, 57, 6965−6972

that its equatorial plane contains five water molecules and that there is no inversion center in $NpO_2(H_2O)_5^+$. As to the 1:1 complex, $NpO_2(L)^+$, the equatorial plane of NpO_2^+ contains two H_2O molecules and one tridentate ligand (Table 2) so that $NpO_2(L)^+$ cannot be centrosymmetric. As a result, both the free $NpO_2(aq)^+$ ion and the 1:1 $NpO_2(L)^+$ complex possess characteristic absorption bands in the near-IR region. In contrast, the 1:2 complex $NpO_2(L)_2^+$ contains two tridentate ligands in the equatorial plane, forming a centrosymmetric structure surrounding the Np center, so that no f−f transitions are allowed and no near-IR absorption is observed.

4. CONCLUSION

In aqueous solutions, the three N-functionalized diacetamide ligands form two complexes with Np(V) with moderate strength, namely, $NpO_2(L)^+$ and $NpO_2(L)_2^+$. The strength of the complexes varies depending on the substituent on the nitrogen atom, following the trend methyl > −H ≈ benzyl. The complexation of NpO_2^+ with the amine nitrogen-linked diacetamides is stronger than that with analogous ether oxygen-linked diacetamide ligand. By integrating the structural information from EXAFS and the theoretical calculation of the energetics, the complexation model that includes the formation of an optically absorbing $NpO_2(L)^+$ complex and an optically nonabsorbing $NpO_2(L)_2^+$ complex is validated.

■ ASSOCIATED CONTENT

Supporting Information

The Supporting Information is available free of charge on the ACS Publications website at DOI: 10.1021/acs.inorgchem.8b00654.

Speciation for EXAFS, experimental conditions of spectrophotometric titrations, and additional computational data (PDF)

■ AUTHOR INFORMATION

Corresponding Authors

*E-mail: lrao@lbl.gov. Phone: +1-510-486-5427. (L.-F.R.)
*E-mail: andrea.melchior@uniud.it. Phone: +39 0432 558882. (A.M.)
*E-mail: lxzhang@lbl.gov. Phone: +1-510-486-5142. (Z.Z.)

ORCID

John Arnold: 0000-0001-9671-227X
Zhicheng Zhang: 0000-0002-2192-3846
Linfeng Rao: 0000-0002-1873-0066

Notes

The authors declare no competing financial interest.

■ ACKNOWLEDGMENTS

This work was supported by the Director, Office of Science, Office of Basic Energy Sciences under U.S. Department of Energy (DOE) Contract No. DE-AC02-05CH11231 at Lawrence Berkeley National Laboratory (LBNL). The EXAFS experiments were conducted at Stanford Synchrotron Radiation Laboratory, a user facility operated for the U.S. DOE by Stanford Univ. Y.G. acknowledges the financial support from the China Scholarship Council for her study at LBNL. The computational work at Univ. of Udine was supported by the "Piano Strategico d'Ateneo 2016-18".

■ REFERENCES

(1) *Yucca Mountain Science and Engineering Report Rev. 1;* U.S. Department of Energy: North Las Vegas, 2002.
(2) Yang, Y.; Zhang, Z.; Liu, G.; Luo, S.; Rao, L. Effect of Temperature on the Complexation of NpO2+with Benzoic Acid: Spectrophotometric and Calorimetric Studies. *J. Chem. Thermodyn.* **2015**, *80*, 73−78.
(3) Zhang, Z.; Yang, Y.; Liu, G.; Luo, S.; Rao, L. Effect of Temperature on the Thermodynamic and Spectroscopic Properties of Np(V) Complexes with Picolinate. *RSC Adv.* **2015**, *5* (92), 75483−75490.
(4) Tian, G.; Rao, L.; Teat, S. J. Thermodynamics, Optical Properties, and Coordination Modes of Np(V) with Dipicolinic Acid. *Inorg. Chem.* **2009**, *48* (21), 10158−10164.
(5) Yang, Y.; Zhang, Z.; Luo, S.; Rao, L. Complexation of NpV Ions with 1,10-Phenanthroline-2,9-Dicarboxylic Acid: Spectrophotometric and Microcalorimetric Studies. *Eur. J. Inorg. Chem.* **2014**, *2014* (32), 5561−5566.
(6) Jensen, M. P.; Nash, K. L. Thermodynamics of Dioxoneptunium-(V) Complexation by Dicarboxylic Acids. *Radiochim. Acta* **2001**, *89* (9), 557−564.
(7) Rizkalla, E. N.; Nectoux, F.; Dabos-Seignon, S.; Pages, M. Complexation of Neptunium(V) by Halo- and Hydroxycarboxylate Ligands. *Radiochim. Acta* **1990**, *51* (4), 113−118.
(8) Eberle, S. H.; Wede, U. Chelatgleichgewichte Fünfwertiger Transurane Mit Aminopolykarbonsäuren. *J. Inorg. Nucl. Chem.* **1970**, *32* (1), 109−117.
(9) Tian, G.; Rao, L. Complexation of NpO_2^+ with N-Methyl-Iminodiacetic Acid: A Comparison with Iminodiacetic and Dipicolinic Acids. *Dalton Trans.* **2010**, *39* (41), 9866−9871.
(10) Ansari, S. A.; Bhattacharyya, A.; Zhang, Z.; Rao, L. Complexation of Neptunium(V) with Glutaroimide Dioxime: A Study by Absorption Spectroscopy, Microcalorimetry, and Density Functional Theory Calculations. *Inorg. Chem.* **2015**, *54* (17), 8693−8698.
(11) Ansari, S. A.; Pathak, P.; Mohapatra, P. K.; Manchanda, V. K. Chemistry of Diglycolamides: Promising Extractants for Actinide Partitioning. *Chem. Rev.* **2012**, *112* (3), 1751−1772.
(12) Tian, G. X.; Zhang, P.; Wang, J. C.; Rao, L. F. Extraction of Actinide(III, IV, V, VI) Ions and TcO_4^- by N,N,N′,N′-Tetraisobutyl-3-Oxa-Glutaramide. *Solvent Extr. Ion Exch.* **2005**, *23* (5), 631−643.
(13) Tian, G.; Xu, J.; Rao, L. Optical Absorption and Structure of a Highly Symmetrical Neptunium(v) Diamide Complex. *Angew. Chem., Int. Ed.* **2005**, *44* (38), 6200−6203.
(14) Dau, P. V.; Zhang, Z.; Dau, P. D.; Gibson, J. K.; Rao, L. Thermodynamic Study of the Complexation between Nd^{3+} and Functionalized Diacetamide Ligands in Solution. *Dalt. Trans.* **2016**, *45* (30), 11968−11975.
(15) Dau, P. V.; Zhang, Z.; Gao, Y.; Parker, B. F.; Dau, P. D.; Gibson, J. K.; Arnold, J.; Tolazzi, M.; Melchior, A.; Rao, L. Thermodynamic, Structural, and Computational Investigation on the Complexation between UO22+and Amine-Functionalized Diacetamide Ligands in Aqueous Solution. *Inorg. Chem.* **2018**, *57* (4), 2122−2131.
(16) Laporte, O.; Meggers, W. F. Some Rules of Spectral Structure. *J. Opt. Soc. Am.* **1925**, *11* (5), 459.
(17) Matsika, S.; Pitzer, R. M. Electronic Spectrum of the NpO_2^{2+} and NpO_2^+ Ions. *J. Phys. Chem. A* **2000**, *104* (17), 4064−4068.
(18) Matsika, S.; Pitzer, R. M.; Reed, D. T. Intensities in the Spectra of Actinyl Ions. *J. Phys. Chem. A* **2000**, *104* (51), 11983−11992.
(19) Matsika, S.; Zhang, Z.; Brozell, S. R.; Blaudeau, J. P.; Wang, Q.; Pitzer, R. M. Electronic Structure and Spectra of Actinyl Ions. *J. Phys. Chem. A* **2001**, *105* (15), 3825−3828.
(20) Infante, I.; Pereira Gomes, A. S.; Visscher, L. On the Performance of the Intermediate Hamiltonian Fock-Space Coupled-Cluster Method on Linear Triatomic Molecules: The Electronic Spectra of NpO_2^+, NpO_2^{2+}, and PuO_2^{2+}. *J. Chem. Phys.* **2006**, *125* (7), 074301.
(21) Rao, L.; Srinivasan, T. G.; Garnov, A. Y.; Zanonato, P. L.; Di Bernardo, P.; Bismondo, A. Hydrolysis of Neptunium(V) at Variable Temperatures (10−85°C). *Geochim. Cosmochim. Acta* **2004**, *68* (23), 4821−4830.
(22) Gran, G. Determination of the Equivalence Point in Potentiometric Titrations. Part II. *Analyst* **1952**, *77* (920), 661.

DOI: 10.1021/acs.inorgchem.8b00654
Inorg. Chem. 2018, 57, 6965−6972

(23) Gans, P.; Sabatini, A.; Vacca, A. Investigation of Equilibria in Solution. Determination of Equilibrium Constants with the HYPERQUAD Suite of Programs. *Talanta* **1996**, *43* (10), 1739−1753.
(24) Ravel, B.; Newville, M. *ATHENA, ARTEMIS, HEPHAESTUS*: Data Analysis for X-Ray Absorption Spectroscopy Using *IFEFFIT*. *J. Synchrotron Radiat.* **2005**, *12* (4), 537−541.
(25) Newville, M.; Ravel, B.; Haskel, D.; Rehr, J. J.; Stern, E. A.; Yacoby, Y. Analysis of Multiple-Scattering XAFS Data Using Theoretical Standards. *Phys. B* **1995**, *208−209*, 154−156.
(26) Lee, C. T.; Yang, W. T.; Parr, R. G. Development of the Colle-Salvetti Correlation-Energy Formula Into A Functional of the Electron-Density. *Phys. Rev. B: Condens. Matter Mater. Phys.* **1988**, *37* (2), 785−789.
(27) Becke, A. D. A New Mixing of Hartree-Fock and Local Density-Functional Theories. *J. Chem. Phys.* **1993**, *98* (2), 1372−1377.
(28) Endrizzi, F.; Melchior, A.; Tolazzi, M.; Rao, L. Complexation of Uranium(VI) with Glutarimidoxioxime: Thermodynamic and Computational Studies. *Dalt. Trans.* **2015**, *44* (31), 13835−13844.
(29) Di Bernardo, P.; Zanonato, P. L. P. L.; Benetollo, F.; Melchior, A.; Tolazzi, M.; Rao, L. Energetics and Structure of Uranium(VI)-Acetate Complexes in Dimethyl Sulfoxide. *Inorg. Chem.* **2012**, *51* (16), 9045−9055.
(30) Grimme, S.; Antony, J.; Ehrlich, S.; Krieg, H. A Consistent and Accurate *Ab Initio* Parametrization of Density Functional Dispersion Correction (DFT-D) for the 94 Elements H-Pu. *J. Chem. Phys.* **2010**, *132* (15), 154104.
(31) Jacobsen, H.; Cavallo, L. On the Accuracy of DFT Methods in Reproducing Ligand Substitution Energies for Transition Metal Complexes in Solution: The Role of Dispersive Interactions. *ChemPhysChem* **2012**, *13* (2), 562−569.
(32) Kuchle, W.; Dolg, M.; Stoll, H.; Preuss, H. Energy-Adjusted Pseudopotentials for the Actinides - Parameter Sets and Test Calculations for Thorium and Thorium Monoxide. *J. Chem. Phys.* **1994**, *100* (10), 7535−7542.
(33) Tomasi, J.; Mennucci, B.; Cammi, R. Quantum Mechanical Continuum Solvation Models. *Chem. Rev.* **2005**, *105* (8), 2999−3093.
(34) Frisch, M. J.; Trucks, G. W.; Schlegel, H. B.; Scuseria, G. E.; Robb, M. A.; Cheeseman, J. R.; Scalmani, G.; Barone, V.; Mennucci, B.; Petersson, G. A.; Nakatsuji, H.; Caricato, M.; Li, X.; Hratchian, H. P.; Izmaylov, A. F.; Bloino, J.; Zheng, G.; Sonnenberg, J. L.; Hada, M.; Ehara, M.; Toyota, K.; Fukuda, R.; Hasegawa, J.; Ishida, M.; Nakajima, T.; Honda, Y.; Kitao, O.; Nakai, H.; Vreven, T.; Montgomery, J. A., Jr.; Peralta, J. E.; Ogliaro, F.; Bearpark, M.; Heyd, J. J.; Brothers, E.; Kudin, K. N.; Staroverov, V. N.; Kobayashi, R.; Normand, J.; Raghavachari, K.; Rendell, A.; Burant, J. C.; Iyengar, S. S.; Tomasi, J.; Cossi, M.; Rega, N.; Millam, J. M.; Klene, M.; Knox, J. E.; Cross, J. B.; Bakken, V.; Adamo, C.; Jaramillo, J.; Gomperts, R.; Stratmann, R. E.; Yazyev, O.; Austin, A. J.; Cammi, R.; Pomelli, C.; Ochterski, J. W.; Martin, R. L.; Morokuma, K.; Zakrzewski, V. G.; Voth, G. A.; Salvador, P.; Dannenberg, J. J.; Dapprich, S.; Daniels, A. D.; Farkas, Ö.; Foresman, J. B.; Ortiz, J. V; Cioslowski, J.; Fox, D. J. *Gaussian 16,* Revision A.03; Gaussian, Inc: Wallingford, CT, 2016.
(35) Tian, G.; Rao, L. Complexation of Np(V) with Oxalate at 283−343 K: Spectroscopic and Microcalorimetric Studies. *Dalt. Trans.* **2012**, *41* (2), 448−452.
(36) Tian, G.; Rao, L.; Xia, Y.; Friese, J. I. Complexation of Neptunium(V) with Fluoride in Aqueous Solutions at Elevated Temperatures. *J. Therm. Anal. Calorim.* **2009**, *95* (2), 415−419.
(37) Rao, L.; Tian, G.; Xia, Y.; Friese, J. I. Spectrophotometric and Calorimetric Studies of Np(V) Complexation with Sulfate at 10−70°c. *J. Therm. Anal. Calorim.* **2009**, *95* (2), 409−413.
(38) Rao, L.; Tian, G. Symmetry, Optical Properties and Thermodynamics of Neptunium(V) Complexes. *Symmetry* **2010**, 1−14.
(39) Tian, G.; Rao, L.; Oliver, A. Symmetry and Optical Spectra: A "Silent" 1:2 Np(V)-Oxydiacetate Complex. *Chem. Commun.* **2007**, *2* (40), 4119−4121.
(40) Neck, V.; Kim, J. I.; Kanellakopulos, B. Solubility and Hydrolysis Behaviour of Neptunium(V). *Radiochim. Acta* **1992**, *56* (1), 25−30.
(41) Combes, J. M.; Chisholm-Brause, C. J.; Brown, G. E.; Parks, G. A.; Conradson, S. D.; Eller, P. G.; Triay, I. R.; Hobart, D. E.; Miejer, A. EXAFS Spectroscopic Study of Neptunium(V) Sorption at the α-FeOOH/Water Interface. *Environ. Sci. Technol.* **1992**, *26* (2), 376−382.
(42) Allen, P. G.; Bucher, J. J.; Shuh, D. K.; Edelstein, N. M.; Reich, T. Investigation of Aquo and Chloro Complexes of UO_2^{2+}, NpO_2^{+}, Np^{4+}, and Pu^{3+} by X-Ray Absorption Fine Structure Spectroscopy. *Inorg. Chem.* **1997**, *36* (21), 4676−4683.
(43) Bessonov, A. A.; Afonas'eva, T. V.; Krot, N. N. Electronic Absorption Spectra of Solid Compounds of Actinoids. IV. Perchlorate, Chloride and Nitrate of Neptunium(V). *Radiokhimya* **1991**, *33* (3), 47−52.
(44) Grigor'ev, M. S.; Baturin, N. A.; Bessonov, A. A.; Krot, N. N. Crystal Structure and Electronic Absorption Spectrum of Neptunyl(V) Perchlorate $NpO_2ClO_4 \cdot 4H_2O$. *Radiokhimya* **1995**, *37* (1), 15−18.

DOI: 10.1021/acs.inorgchem.8b00654
Inorg. Chem. 2018, 57, 6965−6972